Influence of the variation of the content of the sand in the formation of the air bubbles concretes with air-entraining addictive and in the its carbonation

Antonio P. Peruzzi[1]*, Joseph S. Barbar[2], Antonio C. Santos [3], Daniel S. França [4] and Lucas N. Almeida[5]

[1,2,3] Professor Doctor, Faculty of Civil Engineering, Universidade Federal de Uberlandia, Av. Joao Naves de Avila, 2121 - Santa Monica, Uberlandia, Brazil.
[4] Civil Engineering student, Universidade Federal de Uberlandia, Av. Joao Naves de Avila, 2121 - Santa Monica, Uberlandia, Brazil.
[5] Civil Engineering graduate, Universidade Federal de Uberlandia, Av. Joao Naves de Avila, 2121 - Santa Monica, Uberlandia, Brazil.

***Corresponding Author**
Email autor: aperuzzi75@gmail.com

ORCID ID:
A. P. Peruzzi (http://orcid.org/0000-0002-0948-7930)
A. C. Santos (https://orcid.org/0000-0001-9019-4571)

Published: 26 November 2019

Cite this article: Peruzzi, A.P., Barbar, J.S. , Santos, A.C. , França, D.S. & Almeida, L.N. (2019). Influence of the variation of the content of the sand in the formation of the air bubbles concretes with air-entraining addictive and in the its carbonation. *European International Journal of Science and Technology*, 8(10), 1-10.

Abstract
Air-entraining additives are used in civil construction, for an action of elimination of the freeze/thaw cycle, in self supporting concrete and to change its density, to obtain a more economical structure or better thermal performance. Indented characteristics depend on the composition of the raw materials, which in turn depend on the type, quantity and distribution of solids and voids. Granulometric distribution of the sand, have great influence in the formation of the air-entrained bubbles, interfering in the quantity, size and distribution. In this study, were prepared samples using basaltic crushed stone, Portland cement, air-entraining additive (0.5% of the cement mass) with different levels of quartz sand, understand their influence on bubble formation. Thus, 3 types of concretes were studied: A1(1.0:1.0:2.0:0.58); A1.5(1.0:1.5:2.0:0.58); A2.5(1.0:2.5:2.0:0.58) and A3(1.0:3.0:2.0:0.58) (cement:sand:crushedstone:w/c) and casted in cylindrical samples of each of the respective types, cured for 7 days and tested by water absorption, voids index and compressive tests. Amount, size, characteristics of the bubbles entrained into the concretes, were analyzed by optical microscopy. The connectivity of the bubbles formed was studied by exposing the samples in a saturated chamber with CO_2 for 7, 14 and 28 days by the mensuration of the depth of the front of carbonation. The study showed that the variation of the sand quantity used has a great influence on the characteristics of the bubbles formed and, there is a limit that, if exceeded, increases the possibility of its coalescence occurring enabling it's connection, leading to risks related to durability of the concrete.

Keywords: Concrete; Air-entrained; Optical microscopy; Microbubbles; Aggregate variation

Introduction
Air-entraining additives (E_{air}) are used in civil construction, compulsorily for an action of control of the freeze/thaw cycle, but also are used in other types of situations in which the use results in technical advantage like self supporting concrete, or by a lower density to obtain a more economical structure, or better thermal performance. Cast-in-situ reinforced concrete is a good example of this, because has been used in many places around the world as an exterior sealer and represents an economic and quick alternative to masonry or panel systems due to its versatility. Thermal Conductivity (k) of ordinary concrete ranges between 1.4 and 3.6 W/m.K, and that represents a poor thermal performance regarding the building interior. Peruzzi, Rossignolo and Kahn (2018) obtained air-entrained concretes with density 2,040kg/m^3, f_c= 33 MPa and k = 0.72 W/m.K, that match a similar k to ceramic bricks, showing that it is possible to obtain the proper thermal performance for this building system .
Theoretically, the purposely air-entrained bubbles in the concretes are isolated from each other (not connected), this way it does not represent risks to the durability (Neville, 2016). However, there seems to be a limit to the amount of air incorporated (Peruzzi, Rossignolo and Kahn, 2018) because once it is exceeded, the bubbles can rupture or fuse with each other, representing the coalescence phenomena, making the connection possible (Piekarczyk, 2013) and denoting risks to the durability.
On the other hand, several factors interfere at the quantity and quality of bubbles formed by air-entraining additives (E_{air}), such as: the amount of E_{air} additive, type of mixer and mixing time, and the composition of the concrete. Therefore, this paper aimed to analyze the influence of the sand quantity variation on the characteristics, quantity, distribution of the air bubbles and their connectivity. For this purpose, only the proportion of fine aggregate (sand) was varied, while setting fix the type and amount of additive E_{air}, the mixing time and using a single mixer with constant speed. The amount and characteristics of the bubbles formed were studied with the aid of an optical microscope and according to the methodology proposed by Barbar (2016). Connectivity of the air bubbles formed and its

possible compromising effect in the concrete structure durability was studied by exposing the samples in a saturated carbonation chamber of CO_2 (accelerated carbonation) for 7, 14 and 28 days, and the depth of the front of the carbonation was evaluated. The option to use the accelerated process, and the saturated carbonation chamber is based on the fact that a high CO_2 concentration will not change the carbonation process at all, since carbonation will occur instantly, the only effect of the high CO_2 concentration is a faster transport of the CO_2 molecules to the pore air–pore solution interface and thus a faster reaction process (Visser, 2013). Thus, by studying the carbonation front it also was studied the possible connectivity of the bubbles (as already mentioned), and also the durability of concrete.

Experimental Procedure

Materials and Methods

Portland cement (OPC) used for the type III (ASTM C150) has a Density (ρ) of3.12 g/cm³ and F_{c28} = 39 MPa. Quartz Sand used hasρ =2.64 g/cm³ (ABNT NM 52:2009), basaltic crushed stone (#9.5 mm or #3/8")ρ =2.70 g/cm³ (ABNT NM 53:2009). The additive E_{air} used was an aqueous dispersion based on resin acids and rosin acids, fumaric acids and sodium salts, with pH 10 - 12 and ρ varying between 1.010 – 1.050 g/cm^3.

Was prepared four different types of samples of concrete with OPC, sand, crushed stone, w/c 0.58 and 0.5%(cement weight) of additive E_{air}, where upon the amounts of sand varied. These materials were mixed in the mixer for 2 minutes, resulting in the concrete samples A1, A2, A2.5 and A3 their proportions, in weight, is showed at Table 1.

Table 1: Proportions of cement, sand, crushed Stone (in weight) and water/cement of the types of samples

Type of sample	OPC	Sand	Crushed Stone	Water / cement
A1	1.0	1.0	2.0	0.58
A2	1.0	2.0	2.0	0.58
A2.5	1.0	2.5	2.0	0.58
A3	1.0	3.0	2.0	0.58

For each type of sample cylindrical specimens (diameter ϕ = 50mm and height h = 100mm) were prepared as recommended by ASTM C34-13, with a demolding time of 24h, next they were kept immersed in water saturated with $Ca(OH)_2$ for 7 days, to determinate the density (ρ), water absorption ratio, and volume of voids in hardened concrete (ASTM C642-13)three specimens were used for each sample type. Compressive strength was determinated as recommended by ASTM C642-13, using six specimens for each sample type. "Efficiency factor" (EF) has been used to classify a structural lightweight concrete by fc / ρ(MPa.dm^3/kg).

For the optical microscopic analyses, were used two cylindrical specimens of ϕ = 50mm and h = 100mm (for each sample type), from which they were cut at 37.5 mm from the top and at 37.5 mm from the bottom (Fig. 1).

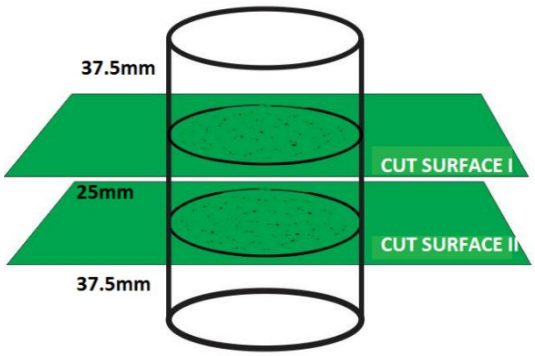

Fig 1 Cut surfaces by circular saw

Specimens with cubic shape 25 x 25 x 25 (mm) were originated (Fig. 2), then the surfaces I and II were marked(on the corresponding cut surface), and the surface I was used for optical microscope analyses.

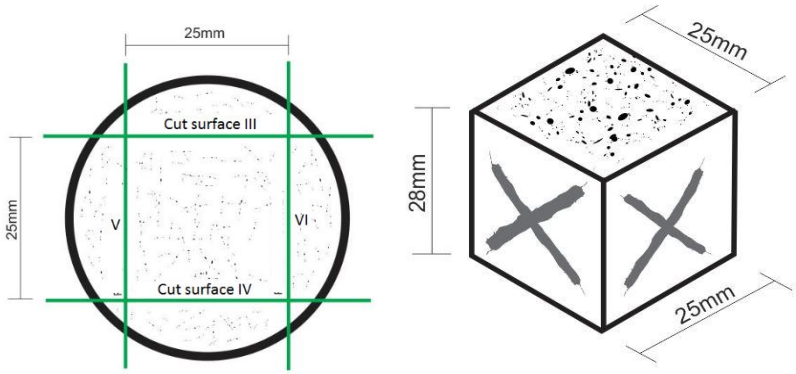

Fig 2 Cut surfaces by circular saw

Using a metallographic sander (150 to 2500 mesh) guaranteed flatness and then the specimens were polished to remove impurities, resulting in cubic specimens and ensuring the desired analysis surface as shown Fig. 3.

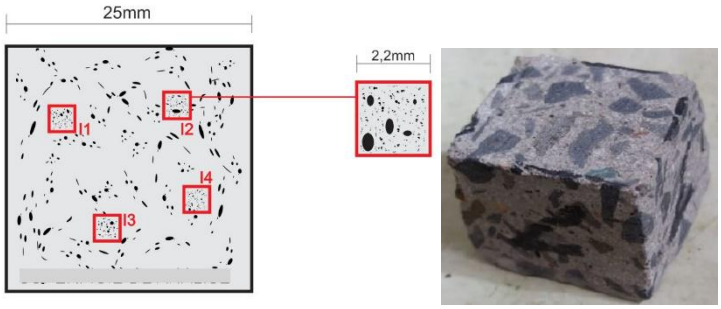

Fig. 3 Example of cubic specimens for the optical microscope

Images acquired by the microscope with a magnification of 50x(Fig. 4), made it possible to observe the bubbles that were delimited, using a Pro Image Express software tool to measure and quantify them for each specific section, according to Barbar (2016).

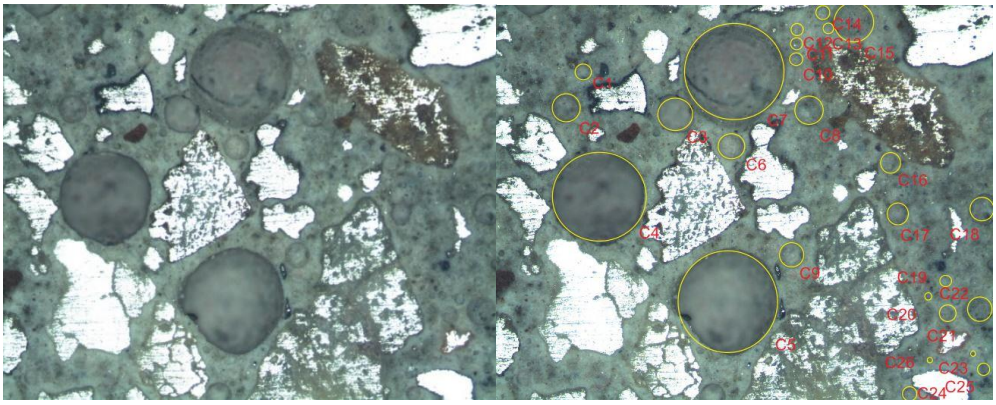

Fig. 4 Scheme of images obtained by software Image Pro Express

The radium of the circumferences was recorded in tables generated by the program itself and later transcribed, obtaining the respective diameters and areas used to obtain and analyze the results.
Accelerated carbonization process began after the wet cure time and when the samples reached a relative humidity of around 35%. They were placed in a hermetically sealed chamber which, after removing the internal air by vacuum, was saturated with carbon dioxide (CO_2), having the uniformity of gas concentration inside the chamber guaranteed by circulation through internal fans. The internal relative humidity was around 70% and the exposure periods used were 7, 14 and 28 days. Then, at the end of each period, each specimen for each type of sample was taken into the chamber and packed with plastic film to prevent moisture loss and possible advancement on the carbonation front by contact with the external environment. All specimens, in their respective exposure time, were ruptured by Tensile splitting (ASTM 496-11) and subsequently sprayed with phenolphthalein solution (pH indicator) (Fig. 5) to allow the determination of the carbonated depth with the aid of a caliper rule.

Fig. 5 Example of cylindrical specimens after ruptured and sprayed with phenolphthalein solution

Statistical analysis

To analyze the statistic validation of the results it was used the Chauvenet criteria.

Results and discussion

Mechanical properties of hardened concrete

Table 2 shows the mechanical properties of the specimens.

Table 2 Density (ρ), absorption after immersion (%), volume of permeable voids (%), compressive strength (fc), efficiency factor (EF)

Type of sample	Density (ρ) (kg/m^3)	Absorption after immersion (%)	Volume of Voids (%)	Fc (MPa)	EF (f_c/ρ) (MPa.cm^3/g)
A1	2,150	8.2	17.6	20.0	9.3
A2	2,050	9.6	19.3	19.4	9.5
A2.5	2,090	8.0	16.7	18.9	9.0
A3	2,030	7.9	16.1	16.8	8.3

Fig. 6 shows the Compressive Strength F_c (MPa) and Efficiency Factor (EF) (MPa.cm^3/g) obtained from samples A1, A2, A2.5 and A3.

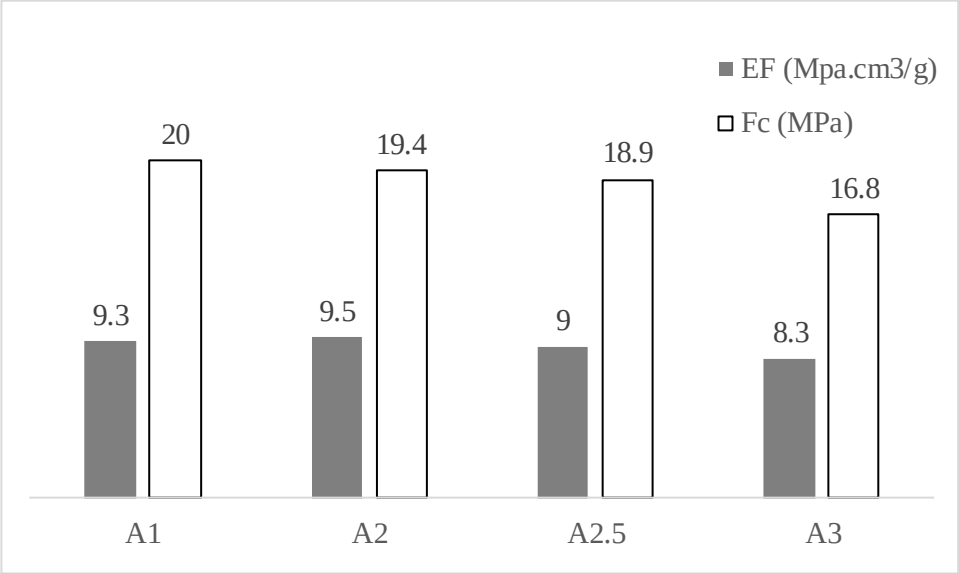

Fig 6 Compressive Strength F_c (MPa) and Efficiency Factor EF (MPa.cm^3/g) obtained from samples

From the results obtained is possible verify that the f_c decreases as the sand quantity increases (Tab 2 and Fig. 6), first because the relation cement/aggregate decreases, but also because a bigger quantity of bubbles were formed, and the decrease of the Density values corroborates that fact (Tab 2 and Fig. 7). However, this tendency is not verified, regarding the density mainly of the sample A2.5 that has a ρ larger than A2. Figure 7 shows Density (kg/m^3), and Fig. 8 shows the Absorption after immersion and Volume of Voids (%) obtained from samples A1, A2, A2.5 and A3.

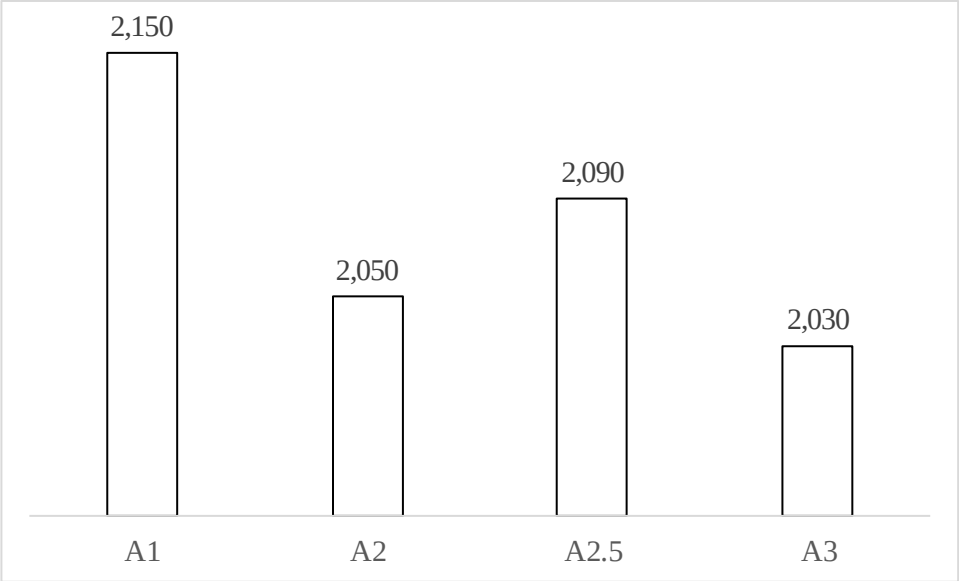

Fig. 7 Density (ρ) (kg/m^3) obtained from samples

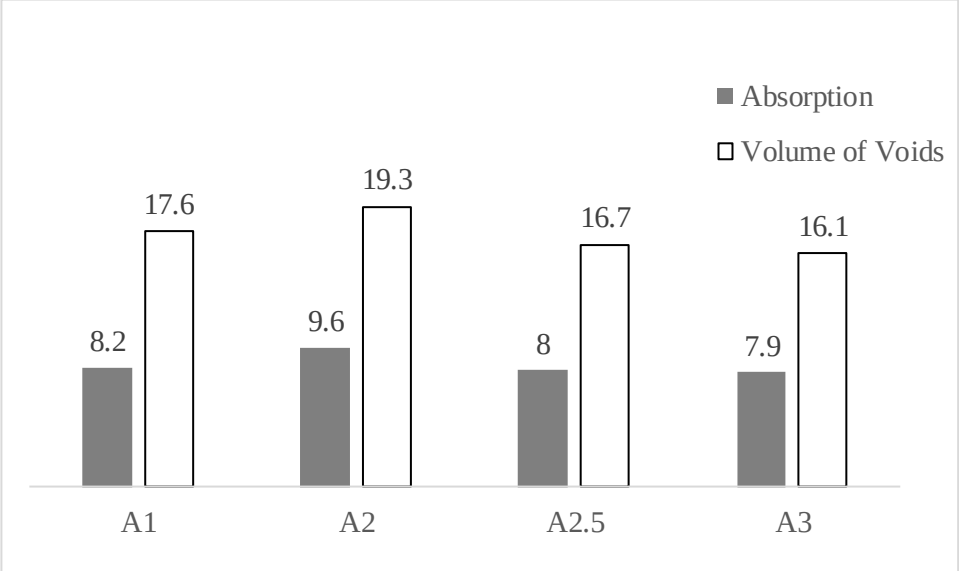

Fig. 8 Absorption after immersion and Volume of Voids (%) obtained from samples

Through the analysis of Figure 8 is possible to note that A2.5 and A3 both have close values of Absorption (8% and 7.9%), but A3 has smaller Density (Fig. 7), and F_c smaller accordingly (Fig. 6), indicating that there are differences in the structure of the bubbles formed, therefore the microstructural analyses can help to understand this process.

Microstructure analysis by Optical Microscope

Table 3 shows the number of bubbles formed, distributed by ranges of Diameter and the total number of bubbles, analyzing the table is possible to note that the number of bubbles increases as the quantity of sand increases, such as expected according to the bibliography.

Table 3 Number of Bubbles (and percentage) obtained from the software Pro Image Express (face I of the prism) distributed by ranges of Diameter and the Total of bubbles

Type of sample	Range of diameter of Bubbles (μm)						Total
	0-100	100-200	200-300	300-400	400-500	>500	
A1	518(91.8%)	38 (6.7%)	5 (0.9%)	1 (0.2%)	0 (0%)	2 (0,4%)	564
A2	80 (55.9%)	41 (28.7%)	12 (8.4%)	2 (1.4%)	2 (1.4%)	6 (4.2%)	143
A2.5	907(88.7%)	83 (8.1%)	18 (1.8%)	7 (0.7%)	1 (0.1%)	7 (0.7%)	1,023
A3	1,056 (90.6%)	72 (6.2%)	19 (1.6%)	3 (0.3%)	1 (0.1%)	14 (1.2%)	1,165

In this paper we detach the range of diameters of the bubbles between two types: 1) "microbubbles" which the diameter is <500μm and the bubbles are considered small, spherical and unconnected, and 2) "macrobubbles" which the diameter is >500μm and they are formed by the mixer or transport of concrete, or product of bubble coalescence. As already said, all of the samples have been made following the same procedures, varying only the sand quantity, so the quantity of "macrobubbles" originated in the mixer phase are, theoretically, the same in all samples, or in other words, the difference of the "macrobubbles" quantity should be product of bubble coalescence. Tab 3 shows that while the quantity of sand increases the "macrobubbles" quantity increases, except in sample A2, that has been showing a different behavior when it comes to Density, Absorption, and number of bubbles. Possibly as a result of the mixing phase. Table 4 shows the Area of the bubbles and the % distributed by ranges of Diameter.

Table 4 Area of the Bobbles (μm^2) x 10^5 (and percentage) obtained from software Pro Image Express (face I of the prism) distributed by ranges of Diameter

Type of sample	Range of diameter of Bubbles (μm)						
	0-100	100 – 200	200 - 300	300 - 400	400 - 500	>500	Area Total (μm^2) x10^5
A1	3.7(35.0%)	2.6 (24.5%)	1.1 (10.4%)	0.6 (5.7%)	0.0 (0.0%)	2.6 (24.5%)	10.6
A2	1.1 (5.4%)	3.1 (15.2%)	2.6(12.7%)	1.0 (4.9%)	1.4(6.9%)	11.2(54.9%)	20.4
A2.5	6.3(18.2%)	6.7(19.3%)	3.5(10.1%)	3.3 (9.5%)	0.7(2.0%)	14.3(42.2%)	34.7
A3	7.0 (22.4%)	4.6 (14.7%)	4.5(14.4%)	1.3 (4.2%)	0.7(2.2%)	13,2(42.2%)	31,3

From Table 4 we can see that the area of "macrobubbles" increases as the amount of sand increases, and the area at A2.5 and A3 have close values, highlighting the coalescence of the bubbles. Whether

this means they are connected or not, and if they can cause durability impairment, can be studied in the Carbonation front analyses.

Carbonation front analyses

Table 5 shows the Carbonation front depth of the samples after 7, 14 and 28 days of Accelerated carbonization placed in a hermetically sealed chamber saturated with carbon dioxide (CO_2). Fig. 9 introduce these results through a bar chart.

Table 5 Carbonation Front Depth (mm) of the samples at 7, 14 and 28 days

Type of sample	Carbonation Front Depth (mm)		
	DaysUnder CO_2		
	7d	14d	28d
A1	1.2	2.5	3.3
A2	3.3	4.3	5.7
A2.5	3.2	5.8	6.5
A3	4.9	6.8	7.0

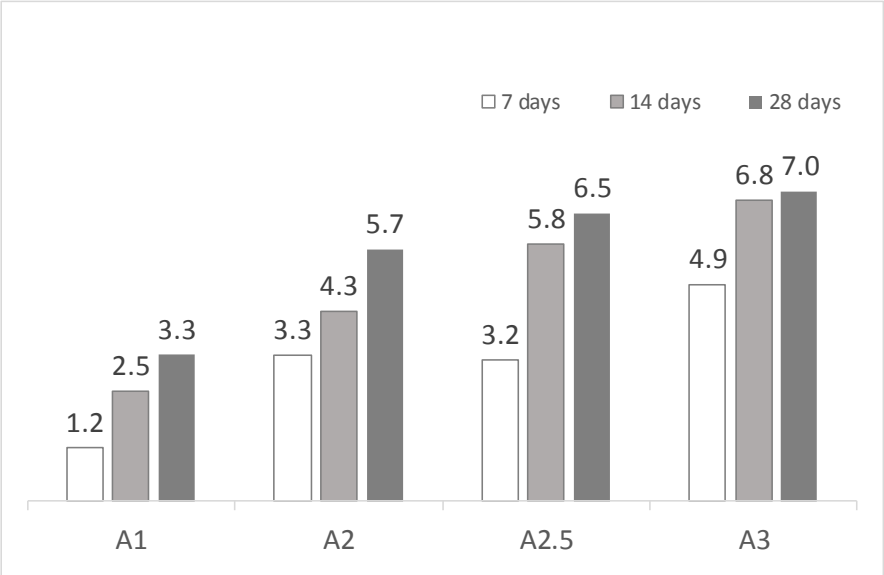

Fig. 9 Carbonation Front Depth (mm) of the samples at 7, 14 and 28 days under Accelerated carbonation process

Tab 5 and Fig. 9 shows that the carbonation front depth increases as the quantity of sand is increased, and denote that there is a connection between the bubbles and sand, and that it may represent risks to the durability of the concrete.

Conclusions

Incorporating sand to the air-entrained concrete significantly increases the quantity of bubbles entrained as the bibliography reports, but it also improves the quality of the bubbles since it is considered that a larger amount of bubbles with smaller diameter is a better condition than one with large bubbles.

The coalescence of the bubbles could be evidenced by the results obtained in this research, mainly related to the number of bubbles and area of the largest bubbles, and their connection by the depth of the Carbonation front.
Results obtained here report that there is a limit to the quantity of bubbles entrained in the concrete and, if exceeded represents risks to the durability of the concrete.

Acknowledgement
The authors thank the Faculty of Civil Engineering of the University Federal of Uberlandia, specially Leticia Silveira Valeriano, Cristiane Pires and Wanderly Geraldo da Silva.

References

[1] Peruzzi, A. P.; Rossignolo, J. A., Kann,H.(2018) Air-entrained concrete: relationship between thermal conductivity and pore distribution analyzed of by X-ray tomography. *Journal of Civil Engineering and Architecture*, http://doi.org/10.17265/1934-7359/2018.07.005

[2] Neville, A. M. (2016) *Propriedades do concreto.* Porto Alegre, RS: Bookman.

[3] Piekarczyk, B. L. (2013) The type of air-entraining and viscosity modifying admixtures and porosity and frost durability of high performance self-compacting concrete. *Construction and building materials,* http://dx.doi.org/10.1016/j.conbuildmat.2012.11.032

[4] Barbar, J. S. (2016) Influência do teor de ar incorporado no desempenho de concretos com diferentes teores de agregados. Doctoral thesis. IAU-SC USP.
https://teses.usp.br/teses/disponiveis/102/102131/tde-23012017-100027/pt-br.php

[5] Visser, J.H.M. Influence of the carbon dioxide concentration on the resistance to carbonation of concrete. Construction and Building Materials. https://doi.org/10.1016/j.conbuildmat.2013.11.005